

# Interference Pattern Formation between Bounded-Solitons and Radiation in Momentum Space: Possible Detection of Radiation from Bounded-Solitons with Bose-Einstein Condensate of Neutral Atoms

Hironobu FUJISHIMA<sup>\*</sup>, Masahiko OKUMURA<sup>1,2,3,4†</sup>, Makoto MINE<sup>5‡</sup> and Tetsu YAJIMA<sup>6§</sup>

*Optics R&D Center, CANON INC., 23-10, Kiyohara-Kogyodanchi, Utsunomiya 323-3298, Japan*

<sup>1</sup>*CCSE, Japan Atomic Energy Agency, 5-1-5 Kashiwanoha Kashiwa Chiba 277-8587 Japan*

<sup>2</sup>*CREST (JST), Kawaguchi, Saitama 332-0012, Japan*

<sup>3</sup>*Computational Condensed Matter Physics Laboratory, RIKEN, Wako, Saitama 351-0198, Japan*

<sup>4</sup>*Computational Materials Science Research Team, RIKEN AICS, Kobe, Hyogo 650-0047, Japan*

<sup>5</sup>*Waseda University Honjo Senior High School, 1136 Nishitomida Honjo Saitama 367-0035 Japan*

<sup>6</sup>*Department of Information Systems Science, Graduate School of Engineering, Utsunomiya University, Yoto 7-1-2, Utsunomiya 321-8585, Japan*

We propose an indirect method to observe radiation from an incomplete soliton with sufficiently large amplitude. We show that the radiation causes a notched structure on the envelope of the wave packet in the momentum space. The origin of this structure is a result of interference between the main body of oscillating solitons and the small radiation in the momentum space. We numerically integrate the nonlinear Schrödinger equation and perform Fourier transformation to confirm that the predicted structure really appears. We also show the simple model which reproduces the qualitative result. Experimental detection of the notched structure with Bose-Einstein condensation of neutral atoms is discussed and suitable parameters for this detection experiment are shown.

KEYWORDS: one-dimensional nonlinear Schrödinger equation, one-dimensional Gross-Pitaevskii equation, radiation, interference, numerical analysis, Bose-Einstein condensation

---

<sup>\*</sup>E-mail address: fujishima.hironobu@canon.co.jp

<sup>†</sup>E-mail address: okumura.masahiko@jaea.go.jp

<sup>‡</sup>E-mail address: mine@waseda.jp

<sup>§</sup>E-mail address: yajimat@is.utsunomiya-u.ac.jp

## 1. Introduction

The one-dimensional nonlinear Schrödinger equation (NLSE),

$$i\psi_t = -\frac{1}{2}\psi_{xx} - |\psi|^2\psi, \quad (1)$$

is a well-known soliton equation which appears in various fields of physics<sup>1</sup> and has many applications such as optical fiber communication.<sup>2,3</sup> Another important example of physical systems for the NLSE is seen in the Bose-Einstein condensation (BEC) of neutral atoms,<sup>4,5</sup> where the macroscopic wave function of condensate atoms appears as the order parameter accompanied with the spontaneous breakdown of the  $U(1)$  gauge symmetry.<sup>6</sup> In this case, the NLSE is regarded as mean-field approximation of the Heisenberg equation for field operators and describes the time-evolution of this macroscopic wave function in good accuracy.<sup>4,5</sup> Up to this day, both bright and dark soliton like objects have been already created with BEC<sup>7,8</sup> (Though, the dark solitons are out of scope of this paper.).

On the other hand, it is clear that we cannot realize rigorous soliton initial condition in any real experiments. However carefully prepared, any realized physical objects must be accompanied with deviation from ideal solitons. Even in such cases, it is widely known that the NLSE has analytical integrability; exact solutions under an arbitrary initial condition is available by the inverse scattering transformation method.<sup>10,11</sup> Especially, to analyze soliton phenomena, we can exploit the Hirota's direct method.<sup>9</sup> It gives us not only the solutions of the NLSE but also clear outlook on classifications of them. It is based on an auxiliary linear eigenvalue problem,

$$\begin{pmatrix} \Psi_{1x} \\ \Psi_{2x} \end{pmatrix} = \begin{pmatrix} -i\zeta & i\psi^* \\ i\psi & i\zeta \end{pmatrix} \begin{pmatrix} \Psi_1 \\ \Psi_2 \end{pmatrix}, \quad (2)$$

where  $\zeta$  is the eigenvalue which is independent of time,  $\psi$  is the solution of the NLSE and asterisk means its complex conjugate. This formulation takes a form of a potential scattering problem for auxiliary field  $\Psi_1$  and  $\Psi_2$  where  $\psi$  works as a potential. The eigenvalue spectrum consists of discrete and continuous parts, where the former generates soliton solutions and the latter corresponds to small ripples called "radiation". For a sech-type initial condition,

$$\psi(x, 0) = M \operatorname{sech}(x), \quad (3)$$

the eigenvalue consists of discrete part only, provided  $M$  equals a positive integer. In this case, whole initial value problem is solved analytically and results in  $M$ -soliton bound state.<sup>12</sup>

Time evolution of the auxiliary field is defined by another linear equation

$$\begin{pmatrix} \Psi_{1t} \\ \Psi_{2t} \end{pmatrix} = \begin{pmatrix} i\zeta^2 - \frac{1}{2}i|\psi|^2 & \frac{1}{2}\psi_x^* - i\zeta\psi^* \\ -\frac{1}{2}\psi_x - i\zeta\psi & -i\zeta^2 + \frac{1}{2}i|\psi|^2 \end{pmatrix} \begin{pmatrix} \Psi_1 \\ \Psi_2 \end{pmatrix}. \quad (4)$$

However, the time evolution of the wave packet from initial conditions except eq. (3) is relatively unclear since analytic treatment of continuous spectrum is hardly accessible. Only we know is asymptotic behavior. According to the analysis of Satsuma and Yajima,<sup>12</sup> a solitary pulse is very robust and unless the spectrum of the eigenvalue problem (2) contains discrete eigenvalue, the wave packet finally splits into soliton part and radiation part. The norm of the soliton part remains  $O(1)$ . When amplitude of the wave packet is large enough, the bounded-soliton can be formed asymptotically and has already been observed in real experiment with optical fibers.<sup>13</sup> In contrast, the amplitude of radiation part decays as  $O(t^{-\frac{1}{2}})$  and expands rapidly from main body of soliton part.

In this way, the amplitude of radiation is generally very small and this makes it difficult to observe radiation in real experiment. In fact, whatever the research field is, any clear observation of radiation has not been reported. Study of radiation has been difficult both theoretically and experimentally, and the problems on the dynamics of the NLSE starting from general initial conditions have not been elucidated.

In this paper, we propose an idea toward experimental observation of radiation through pattern formation in momentum space. We exploit the function of order formation originated with the nonlinearity of the NLSE.

This paper is organized as follows. In the next section, our theoretical idea is explained and the results of numerical simulations are shown. Section 3, the feasibility of real experiment is discussed. The section 4 is devoted to discussion and summary.

## 2. Theory and Numerical Result

In this section, we briefly summarize the mathematical descriptions of the system to be considered. Throughout this paper, we consider the NLSE (1) with initial conditions whose eigenvalue spectrum contain two or more discrete eigenvalues. By virtue of the Galilei transformation, we can restrict ourselves to the case where the center of the wave packet remains at  $x = 0$ . Such situation is achieved as long as the initial condition is real valued and symmetric functions of  $x$ . Under such conditions, the relative velocities of contained solitons vanish and these solitons form bound states.

We consider two similar initial conditions which meet the requirement above. The first is

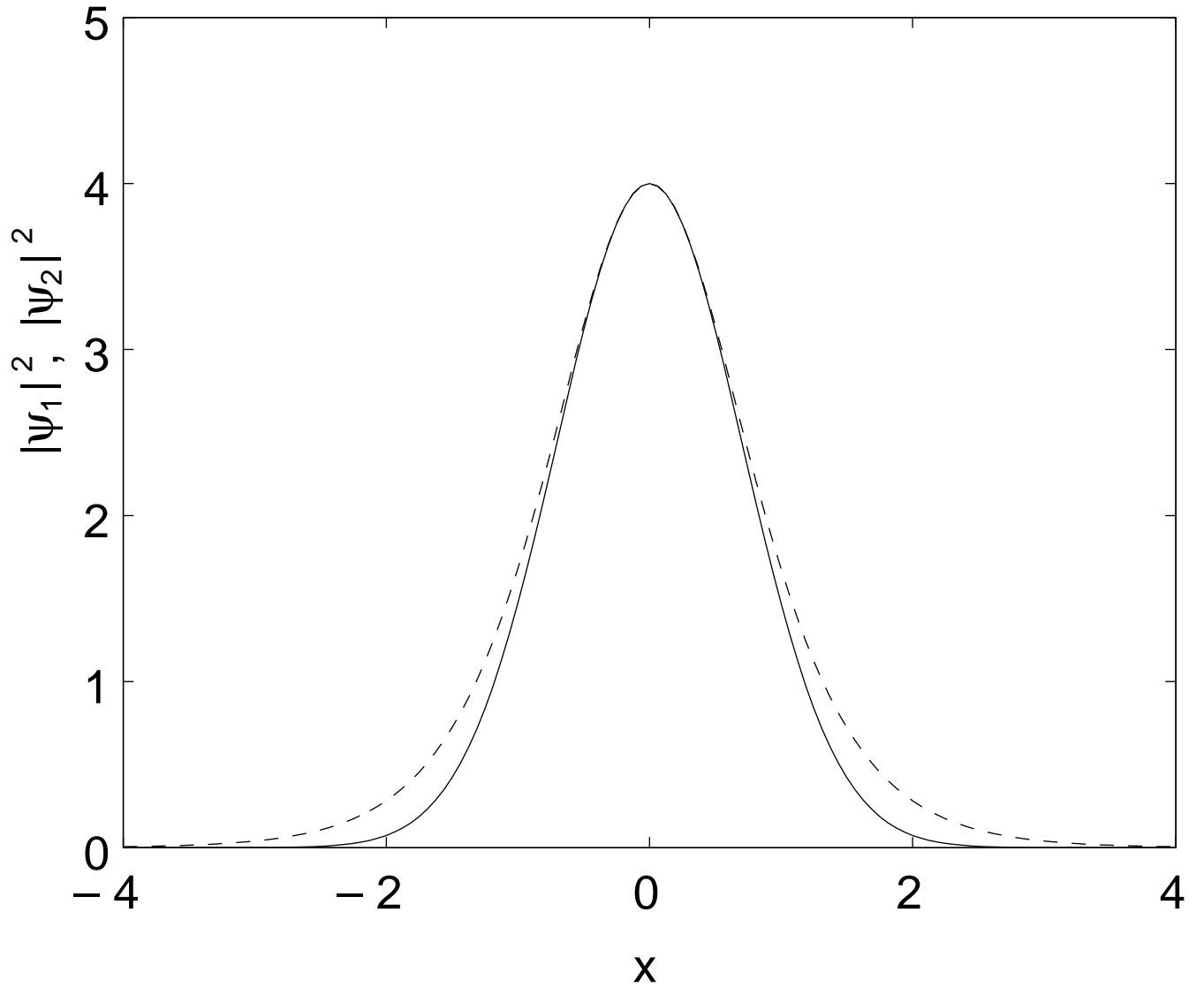


**Fig. 1.** Comparison of the profile of the initial wave packets. The dashed curves for (5) and the solid curve is for (7).

the sech-type (3) one with  $M = 2$ ,

$$\psi_1(x, 0) = 2\text{sech}(x). \quad (5)$$

Starting from  $\psi_1(x, 0)$  results in pure two soliton bound state and this solution reads,

$$\psi_1(x, t) = 4\exp\left(-\frac{it}{2}\right) \frac{\cosh(3x) + 3\exp(-4it)\cosh(x)}{\cosh(4x) + 4\cosh(2x) + 3\cos(4t)}. \quad (6)$$

The envelope of this solution pulsates with the frequency  $\frac{\pi}{2}$  and no radiation is emitted.

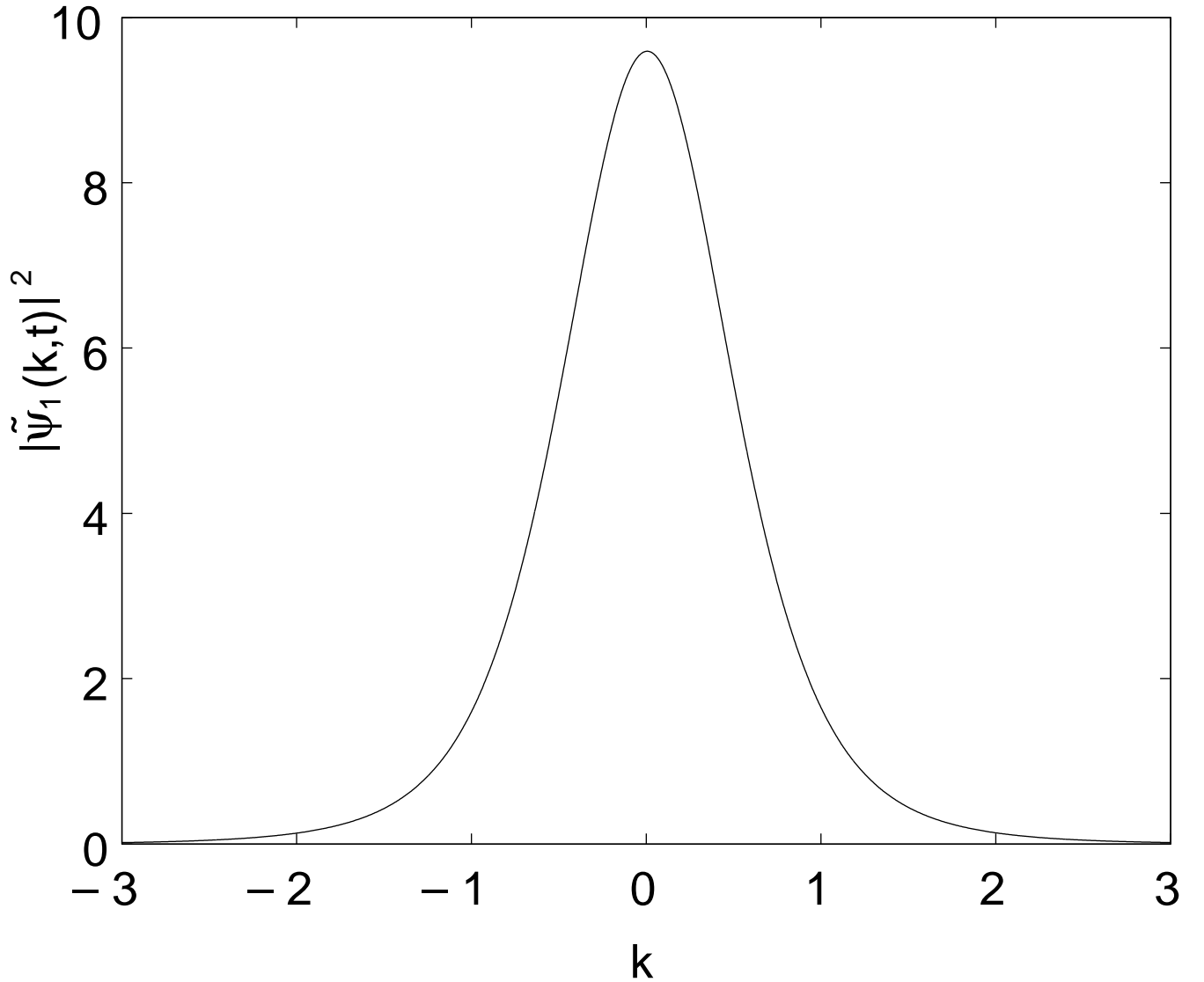


**Fig. 2.** The momentum space profile of the wave packet  $|\tilde{\psi}_1(k, t)|^2$  starting from initial condition (5) at  $t = 14$ .

The second is the Gaussian type with the same amplitude and similar width,

$$\psi_2(x, 0) = 2\exp\left(-\frac{1}{2}x^2\right). \quad (7)$$

This form of initial condition is not only the one that deviates from complete soliton but also one of accessible forms especially in BEC experiments and its time evolution is investigated in detail in our previous work.<sup>14</sup> By the Feshbach resonance technique,<sup>15</sup> we can erase effective inter-atomic interaction. And the atoms trapped in a quadratic potential trap thermalize to form the Gaussian profile. We show  $|\psi_1(x, 0)|^2$  and  $|\psi_2(x, 0)|^2$  in Fig. 1. They have similar figures to each other, in fact, both of them leads to pulsars. However, the wave packet starting

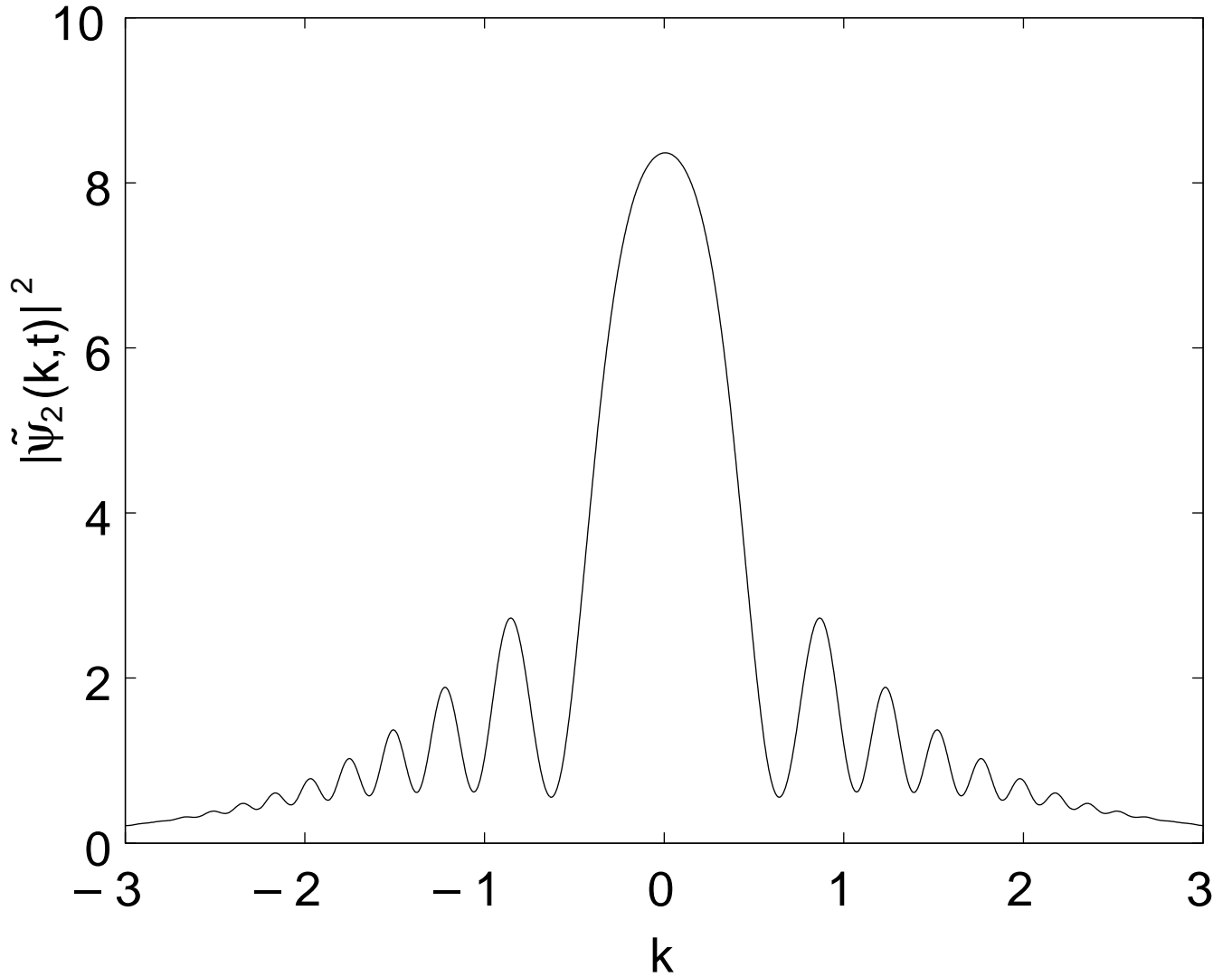


**Fig. 3.** The momentum space profile of the wave packet  $|\tilde{\psi}_2(k, t)|^2$  starting from initial condition (7) at  $t = 14$ .

from the initial condition (7) does not have simple analytical expression and keeps emitting very small radiation which has not been observed experimentally.

We propose a way to distinguish these two initial conditions.

For this purpose, we can find that there appears a distinguishable feature on the envelope of a wave packet which emits radiation. That is a “notched structure” on the envelope in the momentum space. The creation of the notched structure is explained as follows.

When we consider an initial condition with sufficiently large amplitude that deviates from the complete soliton, the total wave function can be expressed as a sum of a soliton part  $\psi_{\text{sol}}$  and a radiation part  $\psi_{\text{rad}}$ , i.e.,  $\psi_{\text{sol}} + \psi_{\text{rad}}$ . We write these two constituent wave functions as  $\psi_{\text{sol}} = g(x)e^{i\theta(x)}$  and  $\psi_{\text{rad}} = h(x)e^{i\theta(x)}$ , where  $g(x)$  and  $h(x)$  are absolute values of  $\psi_{\text{sol}}$

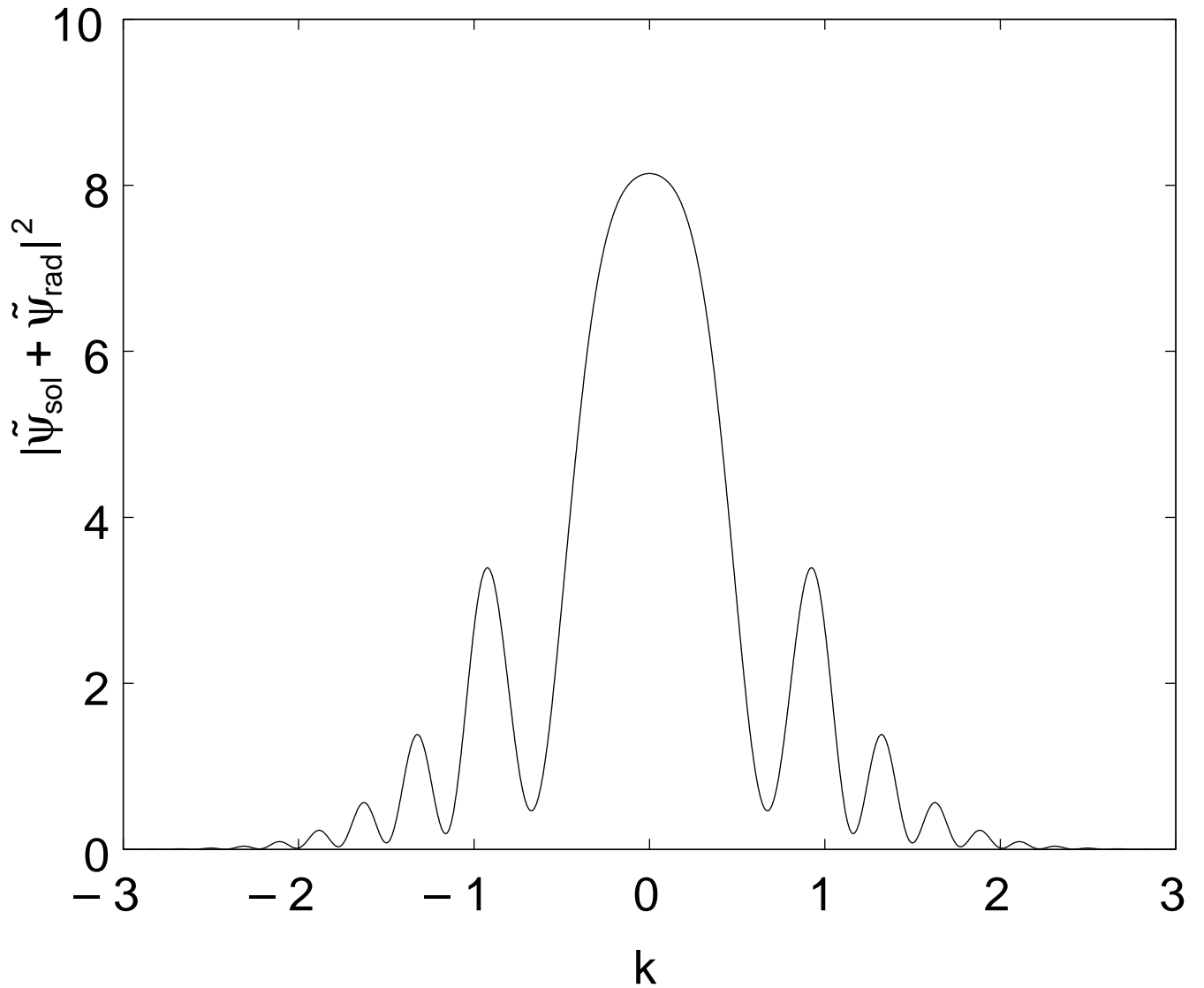


**Fig. 4.** The momentum space profile of the wave packet  $|\tilde{\psi}_{\text{sol}} + \tilde{\psi}_{\text{rad}}|^2$  where  $\tilde{f}(k)$  is taken to be  $e^{-\frac{1}{2}k^2}$ . This snapshot is taken at  $t = 14$ .

and  $\psi_{\text{rad}}$ . They have a definite phase  $\theta(x)$  in common, so that they never interfere with each other in the real space. However, when we perform the Fourier transformation on these wave functions, the difference between  $g(x)$  and  $h(x)$  induces two different phases for  $\tilde{\psi}_{\text{sol}}$  and  $\tilde{\psi}_{\text{rad}}$ , where a tilde means a Fourier component. Now, they can interfere with each other in the momentum space. This interference pattern in the momentum space is nothing else but our notched structure mentioned above and this is an outline of our strategy. Below, we show a brief calculation on the expression of the interference pattern based on a rough but concise model.

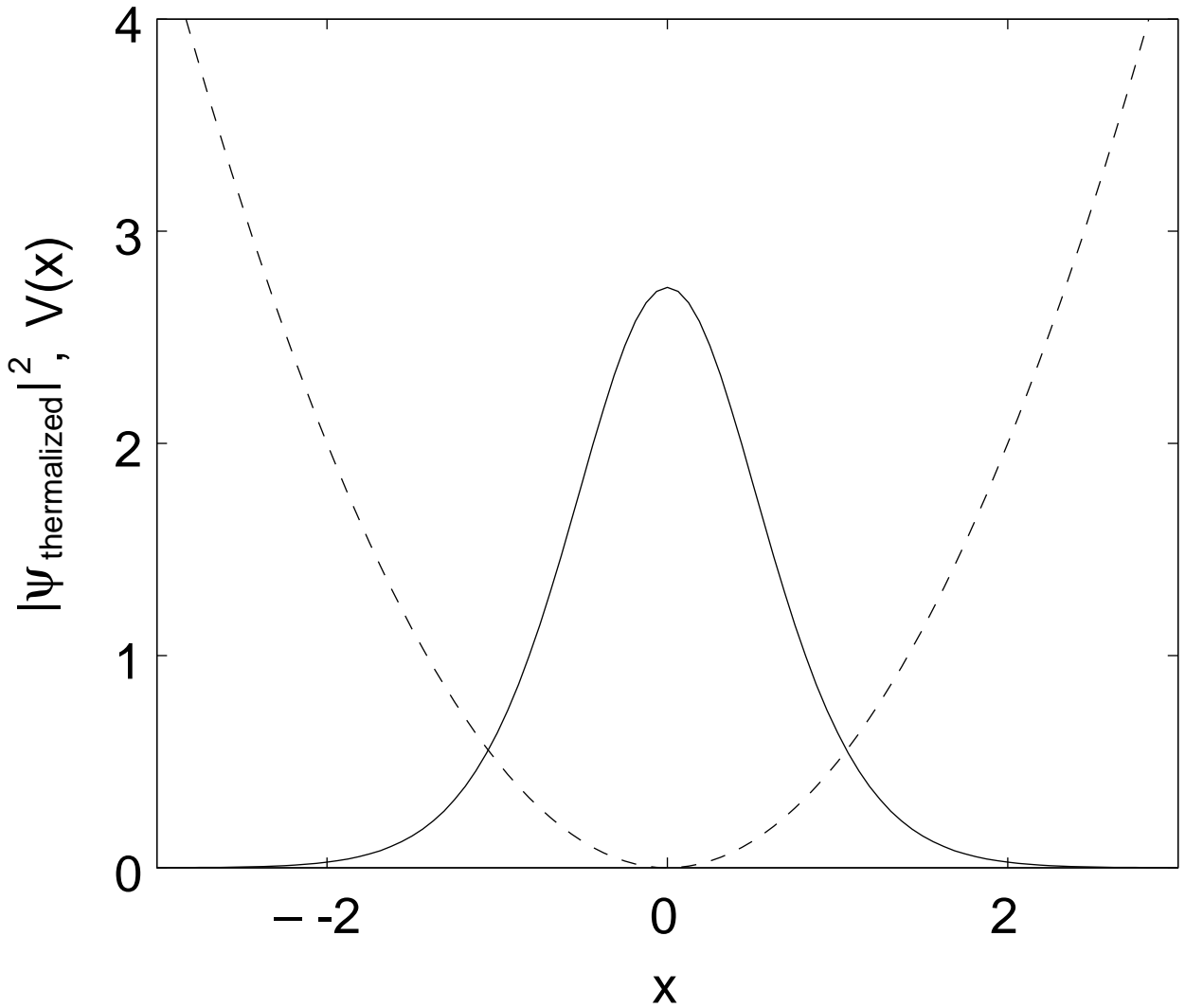


**Fig. 5.** The profile of the wave packet thermalized in the external potential  $V_{\text{ext}}(x) = \frac{1}{2}x^2$ . The real line is for the profile of the wave packet and the dashed line is for the external potential  $V_{\text{ext}}(x)$ .

Since the pulsating soliton part localizes around the origin and oscillates with monochromatic frequency  $\omega = \frac{\pi}{2}$ , it can be approximated as

$$\psi_{\text{sol}}(x, t) = e^{-\frac{1}{2}x^2} (1 + \cos(4t)). \quad (8)$$

We note that this approximation holds for only around the origin, in fact when  $\psi(x, t)$  shrinks, the rest part of the main body of solitons extends toward the left and right to make the whole norm conserved. However, this rather rough approximation does not spoil the qualitative argument because the oscillating amplitude of the side lobe is much smaller than that of the main body of solitons near the origin.

On the other hand, we can neglect the nonlinear interaction term of the radiation part

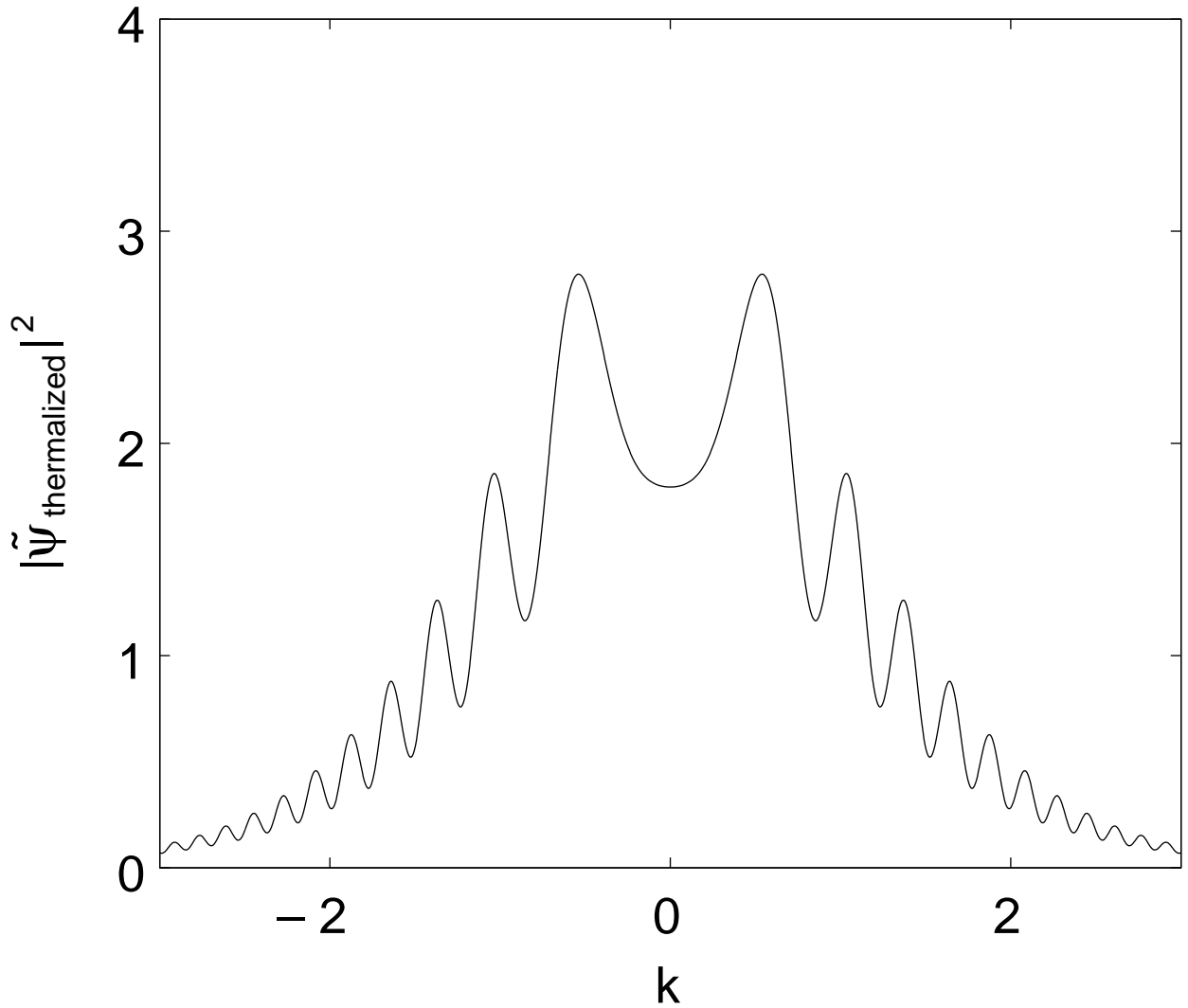


**Fig. 6.** The momentum space profile of the wave packet starting from the one thermalized in the external potential  $V_{\text{ext}}(x) = \frac{1}{2}x^2$ . This snapshot is taken at  $t = 14$  with  $g'_{1D} = 0.7$

because its amplitude is very small. Therefore, the radiation part is well described by the linear Schrödinger equation. Such a wave motion with zero group velocity is expressed as

$$\psi_{\text{rad}}(x, t) = \int \tilde{f}(k) e^{-\frac{i}{2}k^2 t} e^{ikx} dk, \quad (9)$$

where the  $\tilde{f}(k)$  is a real and symmetric function of  $k$ . We shall consider the interfered profile of these two parts in momentum space.

$$|\tilde{\psi}_{\text{sol}} + \tilde{\psi}_{\text{rad}}|^2. \quad (10)$$

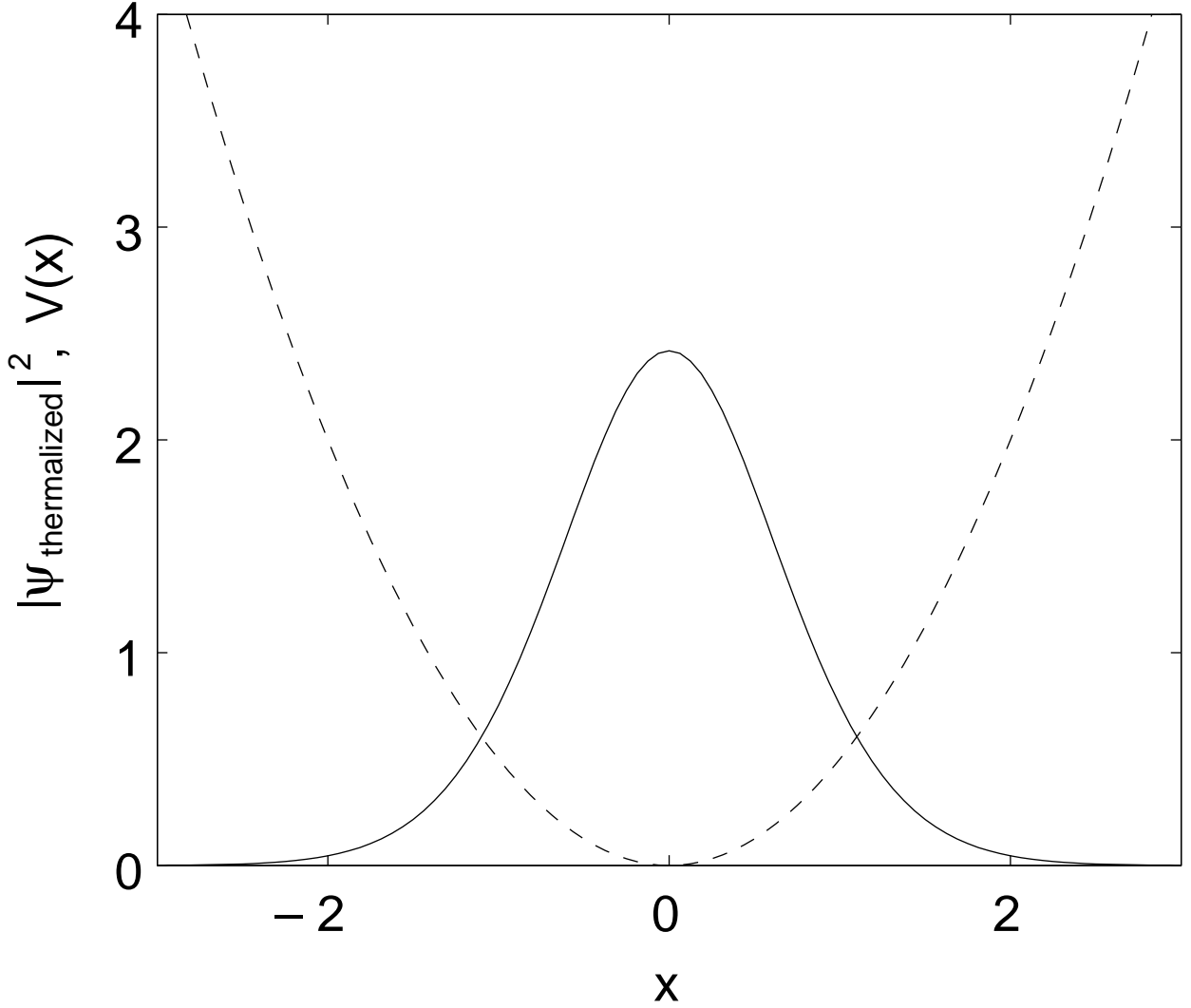


**Fig. 7.** The profile of the wave packet thermalized in the external potential  $V_{\text{ext}}(x) = \frac{1}{2}x^2$ . The real line is for the profile of the wave packet for  $g'_{1D} = 0.7$ , and the dashed line is for the external potential  $V_{\text{ext}}(x)$ .

Obviously, we find  $\tilde{\psi}_{\text{sol}}(k, t) = e^{-\frac{1}{2}k^2} (1 + \cos(4t))$  and  $\tilde{\psi}_{\text{rad}}(k, t) = \tilde{f}(k)e^{-\frac{1}{2}k^2 t}$ . Therefore,

$$|\tilde{\psi}_{\text{sol}} + \tilde{\psi}_{\text{rad}}|^2 = (1 + \cos(4t))^2 e^{-k^2} + \tilde{f}^2(k) + 2(1 + \cos(4t))\tilde{f}(k)e^{-\frac{1}{2}k^2} \cos\left(\frac{1}{2}k^2 t\right). \quad (11)$$

This interference pattern is observed as the notched structure on the surface profile of the wave packet in momentum space. The larger  $k$  makes the oscillation period shorter and the structure is sent out of the center of the profile. This spatial and temporal order is a quite outstanding and it makes it possible for us to observe radiation indirectly.

We show the results of numerical simulation based on the model explained above.

In Fig. 2 and Fig. 3, the snap shot of  $|\tilde{\psi}_1(k, t)|^2$  and  $|\tilde{\psi}_2(k, t)|^2$  are depicted at  $t = 14$ . While the surface of  $|\tilde{\psi}_1(k, t)|^2$  is smooth, the notched structure is fully developed on the surface of

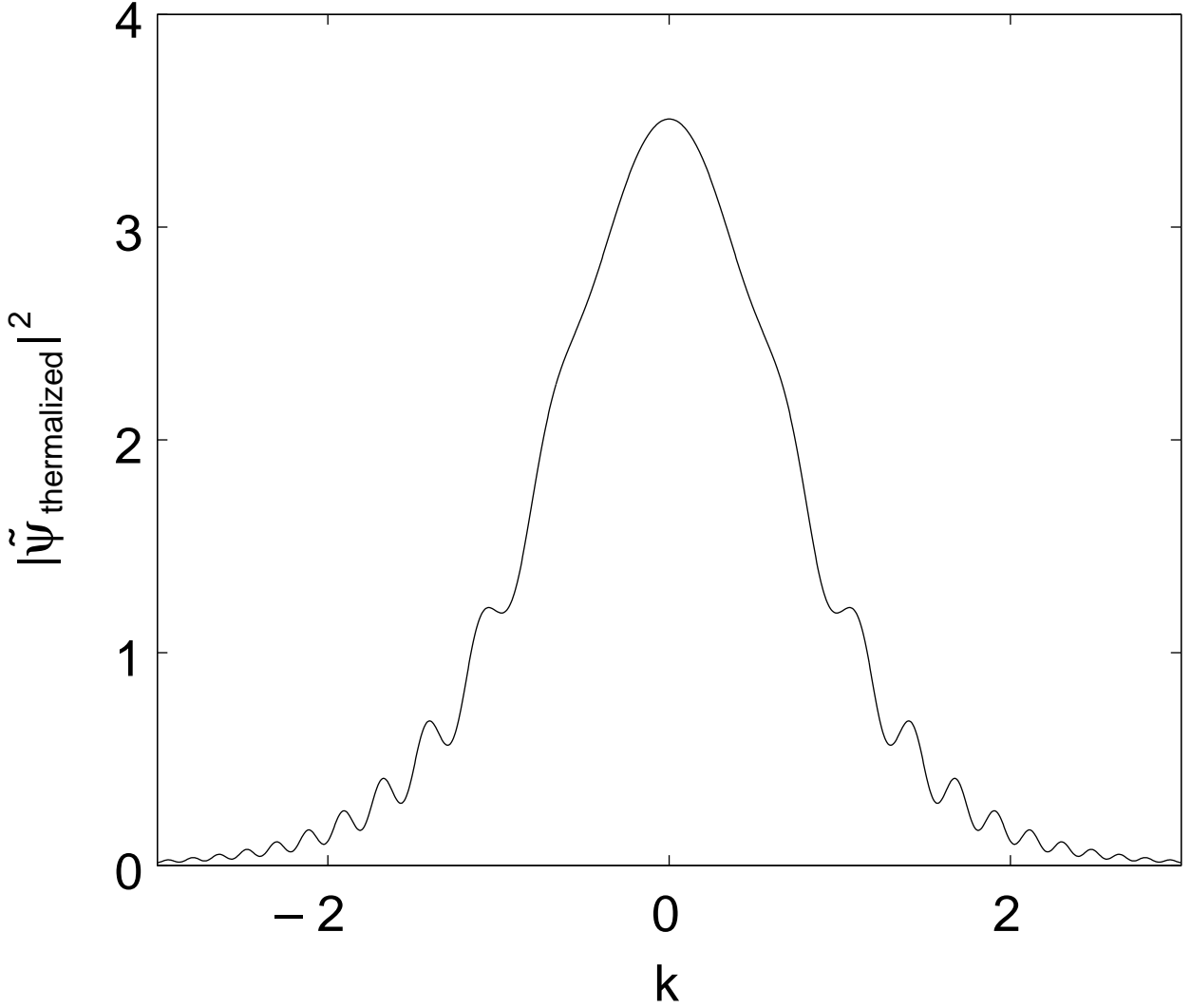


**Fig. 8.** The momentum space profile of the wave packet starting from the one thermalized in the external potential  $V_{\text{ext}}(x) = \frac{1}{2}x^2$ . This snapshot is taken at  $t = 14$  with  $g'_{1D} = 0.7$ .

$|\tilde{\psi}_2(k, t)|^2$ . For reference, Fig. 4 is  $|\tilde{\psi}_{\text{sol}} + \tilde{\psi}_{\text{rad}}|^2$  at  $t = 14$  where  $\tilde{f}(k)$  is taken to be  $e^{-\frac{1}{2}k^2}$ . It is seen that our model qualitatively well describes the result of Fig. 3.

Next, we consider more general case. In real experiments, one usually trap atoms with an external potential  $V_{\text{ext}}(x)$  which can be approximated by a quadratic function. During the trapping time, the macroscopic wave function of atoms gets thermalized. The fully thermalized wave function in the potential corresponds to the initial condition. After this thermalization process in the trapping potential, we switch off the trap and release the atoms to observe interference pattern. Fig. 5 shows the profile of the wave packet thermalized in the external potential  $V_{\text{ext}}(x) = \frac{1}{2}x^2$ . The real line is for the profile of the wave packet and the dashed

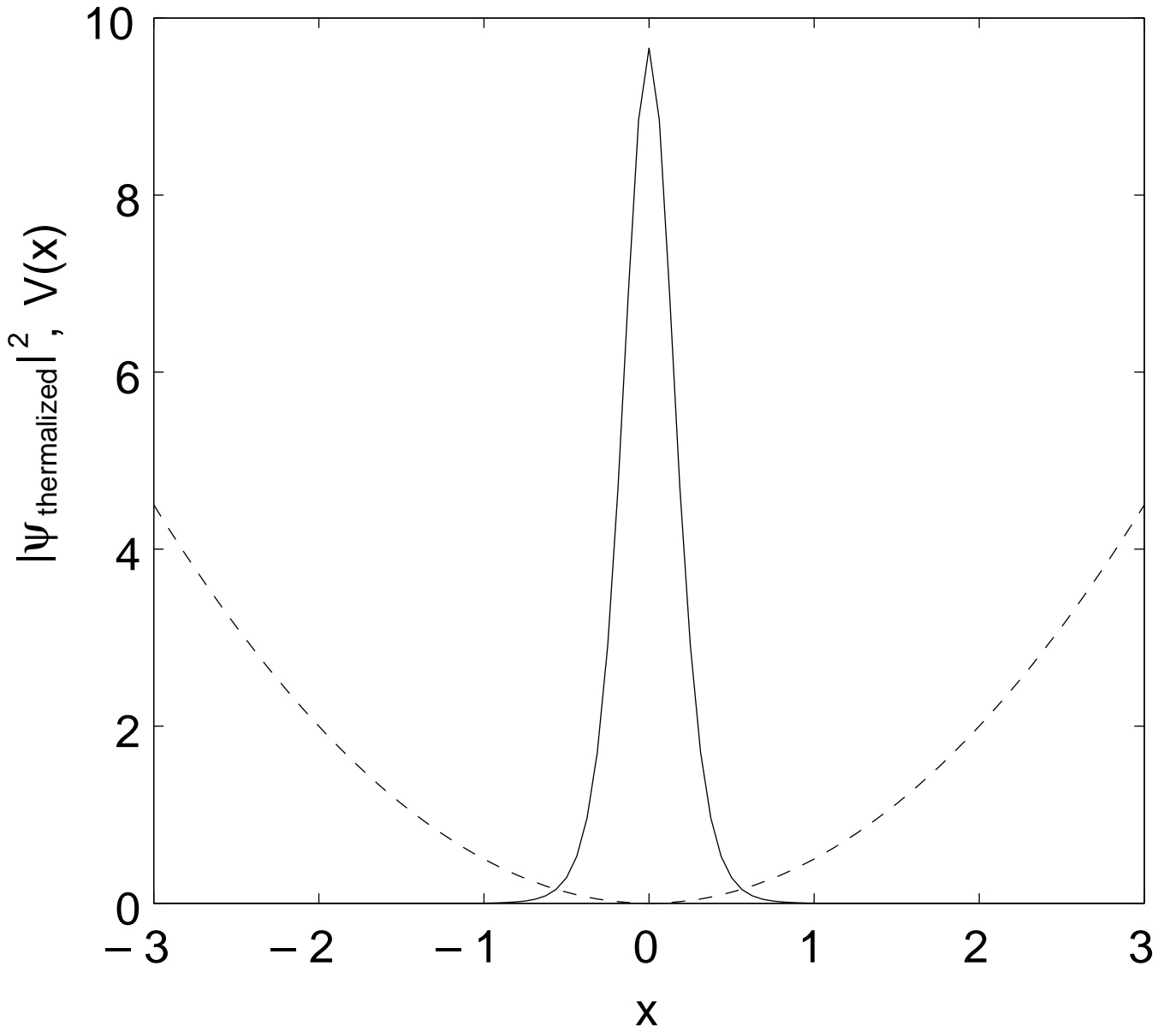


**Fig. 9.** The profile of the wave packet thermalized in the external potential  $V_{\text{ext}}(x) = \frac{1}{2}x^2$ . The real line is for the profile of the wave packet for  $g'_{1D} = 5$ , and the dashed line is for the external potential  $V_{\text{ext}}(x)$ .

line is for the external potential. Fig. 6 is corresponding momentum space profile of the wave packet starting from the one thermalized in the external potential  $V_{\text{ext}}(x) = \frac{1}{2}x^2$ . This snapshot is taken at  $t = 14$ , which is long enough for the wave packets to develop interference pattern. Fig. 6 clearly predicts the emergence of the notched structure from more general initial condition as prepared in realistic experimental setup.

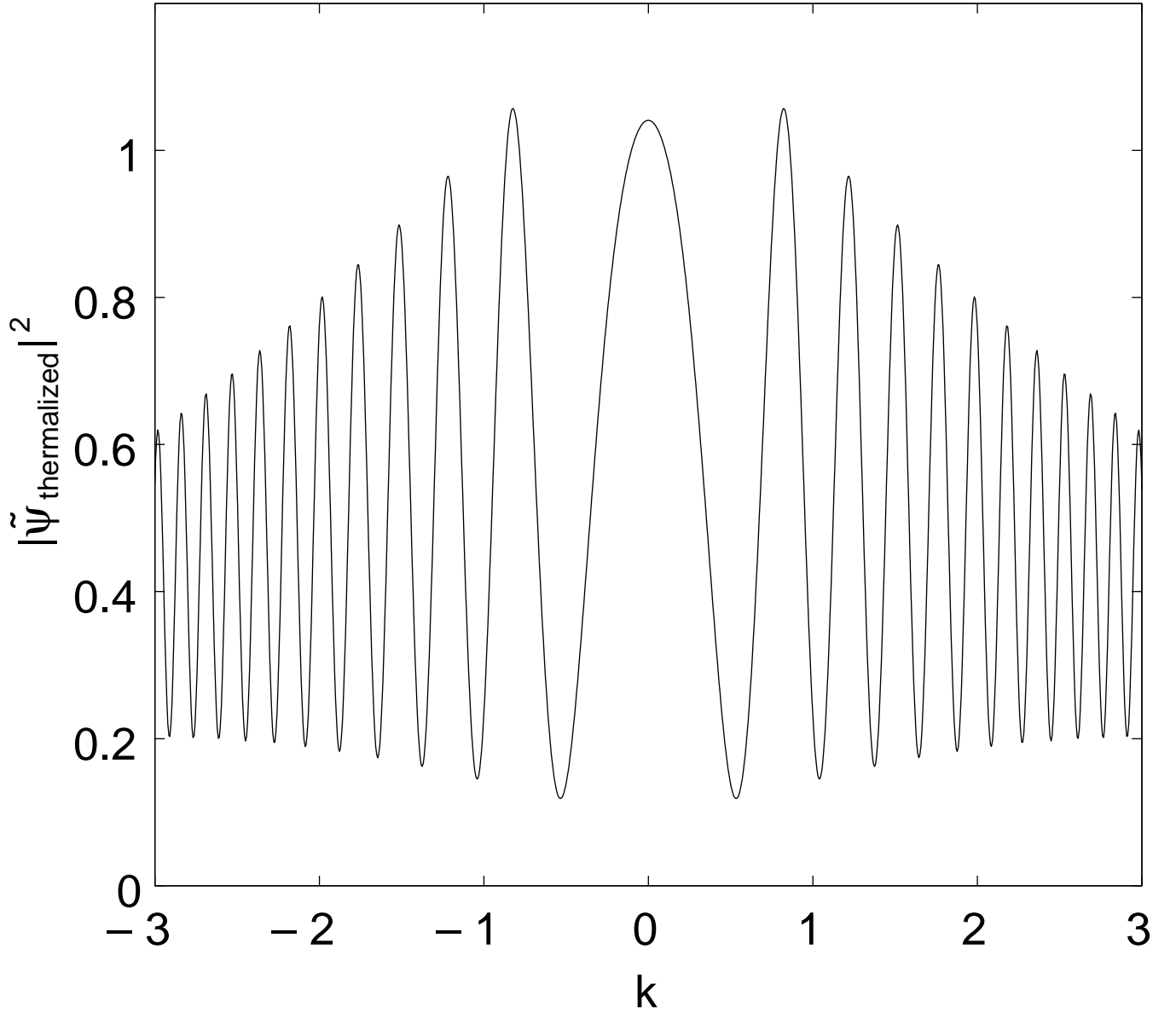


**Fig. 10.** The momentum space profile of the wave packet starting from the one thermalized in the external potential  $V_{\text{ext}}(x) = \frac{1}{2}x^2$ . This snapshot is taken at  $t = 14$  with  $g'_{1D} = 5$ .

### 3. Experimental Feasibility

In this section, we make some remarks on the possibility of real experiments with BEC of neutral atoms. One of the striking feature of BEC experiments is the visibility of the momentum space. One can extract the momentum distribution of cold atoms by the time-of-flight (TOF) method.<sup>16</sup> In the TOF method, while atoms with larger momenta can travel far away, atoms with small momenta can travel only small distances from the origin. Therefore, the momentum distribution is detected directly and we can observe the small radiation ripple

through the formation of interference pattern with the aid of the TOF method. Moreover, the control of external environments is relatively easy in the BEC systems where we can confine condensate particles along quasi rectilinear line by tightening the laser beam trap. Therefore, confirmation of the emitted radiation in BEC experiment is promising. As general requirements for this experiment, we note that sufficient large amplitude is required to form 2-soliton bound state and the strength of the external potential is important. If one uses a too loose potential, the thermalized wave packet might have insufficient amplitude and fail to form 2-soliton bound state. We recommend choosing the coefficient in front of  $x^2$  to be larger than  $\frac{1}{2}$ .

In addition, we need to take special care for some subtleties arising from one dimensional geometry and attractive interaction. In recent paper, Tovbis and Hofer<sup>17</sup> also treated the self-interaction and pattern formation of solitons in similar environment and discussed the possible experimental condition. Although their argument is that in the real space, which is different from our argument in the momentum space, we should also make considerations on the experimental feasibility. To do this task, we rewrite the NLSE (1) back in the original form with dimensional constants as

$$i\hbar \frac{\partial \psi}{\partial t} = -\frac{\hbar^2}{2m} \frac{\partial^2 \psi}{\partial x^2} - g_{1D} |\psi|^2 \psi, \quad (12)$$

where  $\hbar$  is the Dirac constant,  $m$  is the mass of the Bose-condensed atoms and  $g_{1D}$  is the coupling constant. In usual three-dimensional geometry,  $g_{3D}$  is known to be written as  $g_{3D} = \frac{4\pi\hbar^2 |a_{3D}|}{m}$ , where  $a_{3D} < 0$  is the s-wave scattering length of the atoms with attractive interaction. The s-wave scattering length is a quantity peculiar to three-dimensional geometry and it is not a trivial problem to seek for the one-dimensional correspondent. However, in real experiments, we can stay on the NLSE regime provided radial confinement diameter  $a_{\perp}$  is experimentally available level.<sup>18</sup>

The next thing is related to realization of Eq. (1). In usual experiment, we initially trap atoms by applying a harmonic external field and suddenly switch off the trap and release atoms to recover the flat geometry along the axial direction at  $t = 0$ . Strictly speaking, when we use optical trap, a relatively loose Gaussian potential remains along the axial direction even after the release. However, its curvature can be neglected for our purpose. The harmonic external field defines the typical length scale of the system,  $a_{ho} = \sqrt{\frac{\hbar}{m\omega}}$ , where  $\omega$  is the trap frequency. We can reduce (12) to (1) by replacing  $x$  with  $\sqrt{\frac{\hbar}{m\omega}} x$ ,  $t$  with  $\frac{t}{\omega}$  and  $\psi$  with  $\sqrt{\frac{N}{4\sqrt{\pi}}}\psi$ ,

where  $N$  is the total number of particles and by letting  $\frac{Ng_{1D}}{4\sqrt{\pi}\hbar\omega}$  be unity. It follows that

$$N = \frac{4\sqrt{\pi}\hbar\omega}{g_{1D}}. \quad (13)$$

More generally, if we let  $\frac{Ng_{1D}}{4\sqrt{\pi}\hbar\omega}$  be  $g'_{1D}$ , a dimensionless coupling constant, (1) is generalized to be

$$i\psi_t = -\frac{1}{2}\psi_{xx} - g'_{1D}|\psi|^2\psi, \quad (14)$$

and we get

$$N = \frac{4\sqrt{\pi}\hbar\omega g'_{1D}}{g_{1D}}. \quad (15)$$

In real experiment, it would be difficult to adjust  $g'_{1D}$  to exact unity. For such cases, we give here the tolerance for  $g'_{1D}$  to detect desired fringe. Fig. (7) is the profile of the wave packet thermalized in the external potential  $V_{\text{ext}}(x) = \frac{1}{2}x^2$  with  $g'_{1D}$  kept 0.7 and Fig. (8) is the corresponding momentum space profile of the wave packet starting from the one thermalized in the external potential. This is a snapshot taken at  $t = 14$ . It is found that the contrast of the fringe is relatively low because smaller coupling constant  $g'_{1D}$  makes the role of nonlinear oscillation less important. Therefore, we can roughly estimate that the lower bound of suitable  $g'_{1D}$  is about unity.

Coming up next is the upper bound. Fig. (9) is the profile of the wave packet thermalized in the external potential  $V_{\text{ext}}(x) = \frac{1}{2}x^2$  with  $g'_{1D}$  kept 5 and Fig. (10) is the corresponding momentum space profile of the wave packet starting from the one thermalized in the external potential. This is also a snapshot taken at  $t = 14$ . In this case, strong self-focusing interaction makes the initial profile narrower and this leads to a wide-spread profile in the momentum space. In this case, the image intensity in the momentum space would be smaller. We should keep image intensity above detectable level and it defines the upper bound of  $g'_{1D}$ . As a whole, the suitable range for the fringe-detection experiment is roughly estimated to be about  $1 < g'_{1D} < 5$ .

Finally, let us consider preparing the initial condition (7). As mentioned before, we can change the  $g_{1D}$  freely by the Feshbach resonance technique to gain sufficient number of atoms as seen from Eq. (13) and Eq. (15). However, the order of  $N$  is upper-bounded, because this quantity must satisfy the following inequality,

$$N < 0.67 \frac{a_{\perp}}{|a_{3D}|}, \quad (16)$$

to avoid self collapse of condensate due to attractive interaction.<sup>19</sup> In real experiment, Strecker *et al.* used the values  $a_{\perp} \approx 1.5\mu\text{m}$  and  $a_{3D} \approx -0.16\text{nm}$ , letting the order of  $N$  be several

thousand. Therefore, experimental feasibility of our proposal is seem to be promising with the aid of the Feshbach resonance technique provided the number of particles is kept moderate.

#### **4. Summary**

We have proposed an indirect method to observe radiation from incomplete soliton. According to this method, radiation forms the notched structure on the surface profile of the wave packet in the momentum space with the help of the TOF method. The origin of this structure is the result of interference between main body of oscillating soliton and small radiation in the momentum space. We numerically integrated the NLSE and Fourier transformed it to confirm that the predicted structure really appears. Our concept was successfully proved and our simple model reproduced the qualitative result from exact numerical simulation. Finally, we discussed possible conditions required by real experiment with BEC.

#### **5. Acknowledgment**

One of the authors H.F. thanks to the hospitality of Utsunomiya University for offering wonderful working spaces and opportunities of fruitful discussion.

## References

- 1) V.I. Karpman: *Nonlinear Waves in Dispersive Media* (Pergamon Press, Oxford, 1975).
- 2) A. Hasegawa: *Optical Solitons in Fibers* (Springer-Verlag, Berlin, 1990).
- 3) G.P. Agrawal: *Nonlinear Fiber Optics* (Academic Press, San Diego, 1989).
- 4) F. Dalfovo, S. Giorgini, L.P. Pitaevskii and S. Stringari: *Rev. Mod. Phys.* **71** (1999) 463.
- 5) L.P. Pitaevskii and S. Stringari: *Bose-Einstein Condensation* (Oxford University Press, Oxford, 2003).
- 6) M. Okumura and Y. Yamanaka: *Phys. Rev. A* **68** (2003) 013609.
- 7) L. Khaykovich, F. Schreck, G. Ferrari, T. Bourdel, J. Cubizolles, L.D. Carr, Y. Castin and C. Salomon: *Science* **17** (2002) 1290.
- 8) S. Burger, K. Bongs, S. Dettmer, W. Ertmer and K. Sengstock: *Phys. Rev. Lett.* **83** (1999) 5198.
- 9) R. Hirota: *Phys. Rev. Lett.* **27** (1971) 1192.
- 10) C.S. Gardiner, J.M. Greene, M.D. Kruskal and R.M. Miura: *Phys. Rev. Lett.* **19** (1967) 1095.
- 11) V.E. Zakharov and A.B. Shabat: *Sov.Phys. JETP* **34** (1972) 62.
- 12) J. Satsuma and N. Yajima: *Prog. Theor. Phys. Suppl.* **55** (1974) 284.
- 13) L.F. Mollenauer, R.H. Stolen, J.P. Gordon: *Phys. Rev. Lett.* **45** (1980) 1095.
- 14) H. Fujishima, M. Mine, M. Okumura and T. Yajima: *J. Phys. Soc. Jpn* **80** (2011) 084003.
- 15) Ph. Courteille, R.S. Freeland, D.J. Heinzen, F.A. van Abeelen and B.J. Verhaar: *Phys. Rev. Lett.* **81** (1998) 69.
- 16) K.B. Davis, M.-O. Mewes, M.R. Andrews, N.J. van Druten, D.S. Durfee, D.M. Kurn and W. Ketterle: *Phys. Rev. Lett.* **75** (1999) 3969.
- 17) Alexander Tovbis and M.A. Hoefer: *Phys. Lett. A* **375** (2010) 726.
- 18) Kevin E. Strecker, Guthrie B. Partridge, Andrew G. Truscott and Randall G. Hulet: *Nature*. **417** (2002) 150.
- 19) N.G. Parker, S.L. Cornish, C.S. Adams and A.M. Martin: *J. Phys.* **B 40** (2007) 3127.